ELSEVIER

Journal of Electron Spectroscopy and Related Phenomena 117–118 (2001) 57–70

JOURNAL OF ELECTRON SPECTROSCOPY and Related Phenomena

www.elsevier.nl/locate/elspec

Many body effects at surfaces and interfaces

S.D. Kevan[a,*], Eli Rotenberg[b]

[a]*Department of Physics, University of Oregon, Eugene, OR 97403, USA*
[b]*MS2-400, Advanced Light Source, Lawrence Berkeley National Laboratory, Berkeley, CA 94720, USA*

Received 1 August 2000; accepted 20 November 2000

Abstract

The past two decades have experienced the development of angle-resolved photoemission to the point that it can now provide crucial information on an energy scale that is relevant to many key problems in condensed matter physics. At the same time, our ability to prepare and characterize surfaces, interfaces, and thin films has improved to the extent that many exotic phases can be produced with a high degree of perfection. The combination of these two developments suggests many interesting experiments can be performed that probe the coupling between charge, lattice, and spin degrees of freedom in the context of surface and interface physics. In this paper we briefly review a few groundbreaking experiments that have initiated this effort. We also speculate on future developments in this area.

Keywords: Angle-resolved photoemission; Condensed matter; Interface physics; Surface physics

1. Introduction

The most interesting aspect of metals is that at low temperatures the normal metallic state can be unstable due to coupling between the electrons and other excitations in the system. While room temperature properties are well described by treating electrons as independent particles, this paradigm is often called into question when considering the ground state of metals. The reason is that any real system contains not only charge distributions, but also spin and mass (lattice) distributions and these degrees of freedom can mix with the charge to form unusual ground states. For this to happen, a necessary condition is that each distribution is composed of momentum-conserving excitations, and furthermore that these excitations have compatible energy scales. For metals, this latter condition is particularly easy to satisfy since the electronic degrees of freedom can sustain excitations all the way from zero to essentially infinite energy, thereby allowing a coupling to other excitations over a very broad range of spatial and temporal frequencies.

These couplings are found to be most important for low-dimensional systems because the electron density of states becomes progressively more singular at critical points [1,2]. Loosely speaking, having fewer degrees of translational freedom, electrons in low-D systems have fewer ways to avoid coupling to other excitations, and therefore their polarization response to such excitations can become singularly strong. As a consequence of these couplings, the symmetry leading to ordinary room temperature metallic behavior is often unstable with respect to the

*Corresponding author. Tel.: +1-541-346-4742; fax: +1-541-346-3422.
E-mail address: kevan@darkwing.uoregon.edu (S.D. Kevan).

0368-2048/01/$ – see front matter
PII: S0368-2048(01)00245-6

actual, symmetry-broken ground states. This leads to gap formation at low temperatures, with interesting and important ground states such as charge- or spin-density waves. Perhaps the most dramatic example of this situation is observed in conventional superconductivity, which results from a coupling of electrons to phonons. The mechanism for high-T_c superconductivity is still hotly debated; however evidence is growing that it is related to the coupling between two-dimensional electron states and a collective spin excitation [3–6].

The principle types of electronic excitations responsible for symmetry-broken ground states are summarized in Fig. 1 [2]. From the single-particle electron gas dispersion (a) we can derive the two-particle excitation spectrum (b), which shows the allowed energy and momentum changes needed for electron–hole (el–hole) creation. The main point is that there are two classes of low-energy two-particle states which can couple to other low-energy spin and lattice excitations: those with total momentum change $q=0$ and those with $q=2k_F$. Transitions with $q=0$ lead to Cooper pair formation and superconductivity (SC) at low temperature, while $q=2k_F$ transitions lead to electron–hole pairing and hence to charge-density wave (CDW) and spin-density-wave (SDW) formation, depending on whether the dominant coupling is electron–phonon or electron–electron, respectively. In actual materials, the relative coupling strengths determine whether the ground state is CDW, SDW, or SC as shown in the phase diagram (Fig. 1c) [1,2].

The best way to probe the nature of such electron coupling is with a technique that conserves the most important quantum numbers of the system, namely k (wave vector) and s (spin), and that also measures the relevant energies with adequate precision. Finally, detailed temperature dependence is a requirement since much of the interesting physics is thermally driven. Given these requirements, angle-resolved photoemission provides incisive and direct information on quasiparticle lifetimes and dispersion relations. With the advent of new high resolution and high throughput detectors, combined with the availability of third-generation, high brightness light sources, it is now possible to have a complete momentum- and energy-resolved sample characterization in a reasonable period of time. For this reason, the past 5–10 years has witnessed an explosive rebirth of this mature technique as it is being increasingly applied to the highest profile problems in solid state physics.

Over a longer time frame, our ability to prepare and characterize surfaces, interfaces, and thin films has improved to the extent that many exotic phases can be produced, often in situ, with a high degree of perfection. Given the intrinsic reduced dimensionality of a surface or interface and the ability to tailor growth conditions to optimize a particular property, there is every reason to expect that some of these

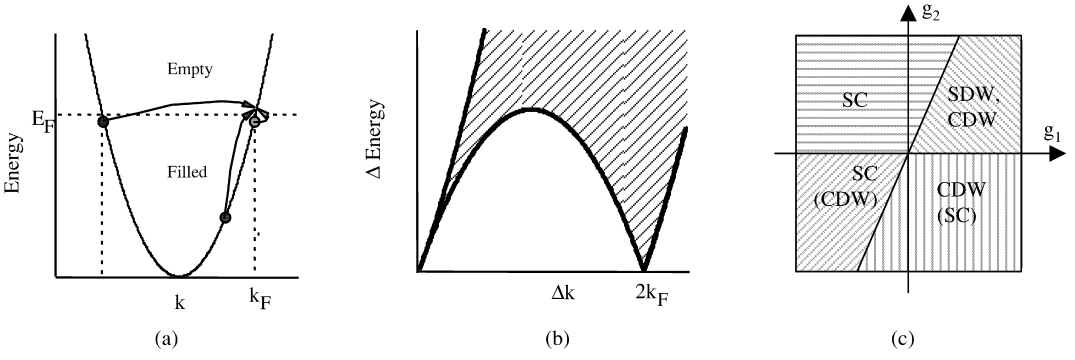

Fig. 1. (a) One-dimensional single-particle band structure, showing possible transitions which create electron–hole pairs. (b) The two-particle excitation spectrum derived from the band structure. Possible excitations are denoted by the shaded area. (c) The one-dimensional phase diagram over the couplings factors g_1 and g_2 at $q=0$ and $q=2k_F$ (from Ref. [1]). Legend: SC = superconducting, CDW = charge density wave, SDW = spin density wave.

surface and thin film phases will exhibit exotic electronic and magnetic phenomena that stem from intrinsically many-body ground states. Moreover, as device sizes shrink, for example, in semiconductor and magnetic materials technologies, understanding and possibly also controlling and using such ground states is a very important goal.

The combination of these two developments — high resolution angle-resolved photoemission and surface/thin film technology — suggests many interesting experiments that probe the coupling between charge, lattice, and spin degrees of freedom in the context of surface and interface physics. In this paper, after a brief discussion of photoemission theory, we review a few groundbreaking experiments that have initiated this process of trying to measure and understand many-body effects at surfaces and interfaces. We close by speculating on the future developments in this area.

2. Photoemission theory

Photoemission is an intrinsically many body process in which, under the influence of a radiation field, an electron is emitted from an interacting N-electron system. The system that is actually measured combines an interacting $(N-1)$-electron or dressed 1-hole state and a freely propagating electron. The measured state is not generally an eigenstate of the $(N-1)$-electron system and thus must be projected onto the true final eigenstates. If one eigenstate dominates, then the state is properly labeled a quasiparticle that has a reasonably well-defined energy, dispersion, etc. Such a state will appear in the photoemission spectrum as a single Lorentzian peak centered at the quasiparticle energy and with a width corresponding to the quasiparticle lifetime — the real and imaginary parts of the quasiparticle self energy, respectively.

The precise relationship between a photoemission spectrum and the underlying spectrum of quasiparticle self energies has been the subject of significant effort over the past three decades, initially through the efforts of Hedin and collaborators [7–9] and later with contributions from others [10–15]. The fundamental understanding of the quasiparticle self energy, of course, is at the heart of much of solid state physics and has been a key focus of quantum field theories of the interacting electron gas since the development of Fermi liquid theory. In this section, we describe the first of these developments in very cursory detail with an emphasis on the relevant approximations made and the information that is in principle available from high resolution, angle-resolved, valence band photoemission. The interested reader is referred to the extensive literature on this subject for details [7–15].

A useful starting point is to express the photocurrent induced by a field of frequency ω (we set $h=1$) in terms of initial and final many body states using the Fermi Golden Rule:

$$J(K, E_K)=2\pi\sum_s |\langle K, N-1, S|\Delta|N, 0\rangle|^2\ \delta(E_K-E_S-\omega). \tag{1}$$

$\langle K, N-1, S|$ is the final state at energy E_K-E_S that includes the emitted electron with momentum K and energy E_K and the $(N-1)$-electron state left in state S. Δ is the Hamiltonian describing the interaction of the radiation field with the N electrons and normally neglects the spatial variation of the field. $|N, 0\rangle$ is the initial N-electron state, assumed for simplicity to be the ground state and for convenience to have zero energy. A key approximation often made to simplify this expression is that the final state can be factored into independent photoelectron and photohole states. The validity of this approximation rests in part with the sudden approximation, which assumes the photoelectron is decoupled from the $(N-1)$-electron state and thus carries no information about it. This approximation has been adequately tested at the relatively high excitation energies associated with X-ray photoelectron spectroscopy [16]. Few tests have been made at the lower energies normally used in valence band photoemission, and the approximation sometimes remains an issue [17,18]. The approximation of independent photoelectron and photohole states also ignores extrinsic losses suffered by the photoelectron after the excitation event.

We choose a suitable basis of one-electron orbitals judiciously labeled with the index k_i and of energy ε_i. This set will describe the one-electron band structure that is renormalized by many body effects as it is mapped into the observed photoemission spectrum. Applying the above approximation to the

Golden Rule expression, it is straightforward to show that the photocurrent may be written in terms of a sum over dipole matrix elements Δ_{if} between initial and final orbitals and the spectral function of the photohole state, $A(k_i, \varepsilon)$: [7–15,18]

$$J(K, E) = \sum_i |\Delta_{if}|^2 A(k_i, \varepsilon) \tag{2}$$

where $\varepsilon \equiv E_K - \omega$ is the photohole energy relative to the Fermi level. The spectral function is related to the single particle Green function that plays a key role in many body treatments of the interacting electron gas:

$$A(k_i, \varepsilon) = \frac{1}{\pi} \operatorname{Im} G(k_i, \varepsilon) = \frac{1}{\pi} \frac{|\operatorname{Im} \Sigma(k_i, \varepsilon)|}{(\varepsilon - \varepsilon_i - \operatorname{Re} \Sigma(k_i, \varepsilon)) + (\operatorname{Im} \Sigma(k_i, \varepsilon))^2} \tag{3}$$

For example, the spectral function for independent particles is $A(k, \omega) = \delta(E_K - \omega - \varepsilon)$, and the photocurrent is given by the well-known one-electron expression.

The above formalism is general, though it has been developed and until fairly recently applied primarily to treat core level photoemission spectra and the associated intrinsic shake-up and plasmon satellite structures [10,16]. Within the realm of validity of the sudden approximation, however, it is equally applicable to valence band spectra. In the case of a perfect crystalline solid, the matrix element provides conservation of momentum parallel to a surface plane. For the two-dimensional states of primary interest here, the sum collapses into a single term at a value of parallel momentum $k_{||}$ that is determined by the polar emission angle and kinetic energy through a simple kinematic relationship:

$$k_{i,\|} = \sqrt{\frac{2mE_K}{\hbar^2}} \sin\theta \tag{4}$$

The observed spectrum is given by a matrix element at the selected parallel momentum multiplied by the photohole spectral function at the same momentum. It is normally assumed that the matrix element varies smoothly and slowly as a function of energy and momentum, so the measured photoemission spectrum reflects directly the shape of the spectral function. Therefore, given approximate particle–hole symmetry about the Fermi level, measuring this single-particle spectral function using photoemission provides a unique and incisive probe of the underlying interactions that dress the quasiparticle and determine its self-energy. The situation for three-dimensional states is more complicated since damping of the photoelectron state implies that the momentum normal to the surface is not precisely conserved. In either case, however, ε_i corresponds to a one-electron band energy. The real and imaginary parts of the self-energy are seen to represent the energy shift and broadening of the observed quasiparticle peak in the photoemission spectrum. In many situations, the single-particle bands of key interest lie at or near the Fermi level. By changing the parallel wave vector, one can probe systematically how the spectral function varies in the vicinity of the Fermi level.

A detailed description of the self-energy of an interacting electron gas is beyond the scope of our review, and the interested reader is referred elsewhere for details [9,19,20]. Before proceeding with a discussion of various experiments that use this phenomenology, however, it is useful to discuss briefly and qualitatively the contributions to the self-energy. Various scattering processes determine the self-energy: electron–phonon, electron–electron, electron impurity, electron–magnon, etc. Each of these has a characteristic interaction strength and energy scale. The electron–phonon coupling parameter λ and the Debye energy ω_D, for example, are two simple parameters that characterize the scattering of electrons or holes by acoustic phonons. If the energy scale of two interactions is widely different, then their contributions are often not strongly coupled. As a first approximation, the various contributions to the self-energy may simply be summed: [19]

$$\Sigma = \Sigma_{imp} + \Sigma_{ph} + \Sigma_{e-e} + \cdots \tag{5}$$

Even with this separation into contributions from individual process, it is difficult to isolate the impact of one from all the others. It is important to realize, for example, that the one-electron energies ε_i cannot be measured and, indeed, are really just a convenient mathematical construct. Re Σ measures the difference between the measured quasiparticle energy and

something that at best can only be calculated. Of course, finite experimental energy and momentum resolution serve to complicate further the extraction of useful parameters to describe many body interactions from photoemission data.

Despite this difficulty, it is now apparent that good progress can be made since the various contributions generally impact the self-energy in different ways and often on different energy scales. Evidence for this observation is provided in the following sections, but let us first enumerate how these contributions impact the total self-energy. Im Σ_{e-e} has an energy-dependent form that is nominally proportional to ε^2, though the precise form depends on dimensionality. Re Σ_{e-e} is generally predicted to be smoothly varying, the main impacts being on overall band width, band mass, and Fermi velocity [17,19]. For single band systems, the Fermi wave vector is not altered by this or any other many body interaction. Σ_{imp} is nearly pure imaginary and constant [21]. It clearly will depend on the quality of material used, which is often difficult to control for surfaces and thin films. Both the real and the imaginary parts of Σ_{ph} are structured on an energy scale comparable to a characteristic phonon energy (e.g., ω_D) [22]. To reiterate, the impact of electron–electron interactions occurs on an energy scale of ~1 eV and provides a smooth deviation of the quasiparticle peaks from the one-electron bands. Impurity scattering provides an approximately constant imaginary contribution and can be reduced by improved sample preparation. The impact of the electron–phonon interaction tends to saturate at large hole energy, but can dramatically influence the spectral function for energies less than a characteristic phonon energy (e.g., ω_D).

3. Examples

3.1. Electron–electron self energy in bulk sodium

Before pursuing our main subject, that is, many body effects at surfaces and interfaces, it is useful to examine a simple bulk system where the impact of Σ_{e-e} is readily apparent. We turn to experiments that measured the quasiparticle dispersion relation the of sodium 3*s* band [23,24]. Sodium is a classic free-electron metal where simple models explain a variety of different observations. It is, therefore, surprising that a large theoretical effort has been spawned to explain their deceptively simple results. Jensen and Plummer did not measure Im Σ_{e-e} since information about this is masked by scattering of the final state photoelectron. Nonetheless a simple procedure was adopted to measure the quasiparticle dispersion relations in 'absolute' fashion, and thereby to extract information about Re Σ_{e-e}.

Their measured dispersion relation is plotted in Fig. 2 along with a one-electron band calculated in the local density approximation. The occupied portion of this calculated band is essentially the same as the free electron (Sommerfeld model) band. The LDA effective mass is the same as the free electron

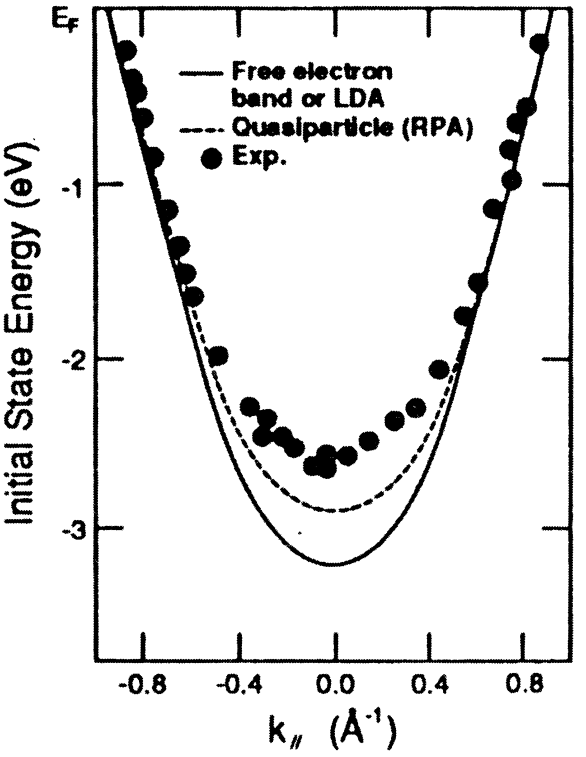

Fig. 2. Experimental quasiparticle dispersion relations for the 3*s* band of sodium, taken from Ref. [24]. The solid curve is both the free-electron (Sommerfeld result) and that produced by modern LDA calculations. The dashed curve (taken from Ref. [25]) is for jellium of the appropriate density and includes many body effects at the level of RPA. The shift between the experimental points and the independent electron result is a direct measure of the real part of the electron–electron self energy.

mass, and the occupied band width is 3.2 eV. By contrast, the measured quasiparticle band has a fitted effective mass of 1.23 times the free electron mass, and the band width is 2.5 eV [24]. The difference between these two dispersion relations provides a direct measure of Re Σ_{e-e}, assuming the calculation provides a reasonable description of the one-electron bands. As noted above, the impact of Re Σ_{e-e} is smooth and occurs on an energy scale comparable to the band width. Also, the Fermi wave vector of the one-electron band is the same as that of the quasiparticle dispersion relation.

Attempts to model these results by calculating Im Σ_{e-e} have met with varying degrees of success, an example of which is shown by the dashed curve in Fig. 2 [25]. These efforts have been adequately reviewed elsewhere [12] and, moreover, are not particularly germane to our emphasis in the present review. We emphasize, however, that such renormalization of occupied quasiparticle band widths, band masses, and band gaps due to the electron–electron self energy is a very common phenomenon. For example, a recent experiment on $TiTe_2$, a quasi-2D material that allows the full power of the photoemission technique to be exercised, came to similar conclusions about Re Σ_{e-e} and, moreover, also measured and analyzed Im Σ_{e-e} [17,18]. That experiment provided strong support of the phenomenology of applying single particle spectral functions to interpret valence band photoemission spectra.

The key point we want to make concerns the possible measurement of other contributions to the self energy. In principle, the impact of Σ_{imp} could be measured by additional broadening in the raw spectra. Also, Σ_{ph} should induce structure in the quasiparticle dispersion relation very close to the Fermi level, similar to that explored in the following sections. However, the observed photoemission line widths are dominated by scattering of the final state photoelectron, which endows the experiment with fundamental broadening on the scale of ~1 eV. Both of these other screening mechanisms occur on a much smaller energy scale and therefore cannot be measured in these experiments on alkali metals. In a 2-D system (as was the case for $TiTe_2$ noted above and in the experiments discussed below), this broadening mechanism is not relevant [26]. Within the approximation of additive contributions to the self-energy, when considering the electron–phonon interaction, for example, the 'one-electron band' should actually be taken as the band that has been renormalized by the higher-energy electron–electron interaction. In all the cases discussed below, this Re Σ_{e-e}-renormalized band dispersion, labeled ε_i in Eq. (3), is determined at 'high' hole energy ($\varepsilon \gg \omega_D$) and extrapolated through the Fermi level.

One conclusion to be drawn from this is that it is often better to measure Re Σ through modified or perturbed quasiparticle dispersion relations than to measure Im Σ through careful analysis of photoemission line widths. This is true even though these quantities are fundamentally related by Hilbert (Kramers–Kronig) transformation. Our reasoning is that the contributions to Im Σ add throughout the spectra, while the contributions to Re Σ tend to be localized over particular ranges of energy and thus are more easily separated.

3.2. Phonon scattering on Cu (111)

The very well-known surface state located near the center of the surface Brillouin zone (SBZ) on Cu(111) has provided an excellent testing ground for many aspects of surface electronic structure, including the impact of impurity and phonon scattering [27–29]. The state exists in a projected gap in the bulk band structure defined by the neck of the bulk Fermi surface near the L symmetry point. The measured dispersion relation forms an isotropic paraboloid about the center of the SBZ with an effective mass of 0.42 times the mass of the electron. Spectra from an early high resolution measurement of this state are presented in Fig. 3 [27]. The parabolic dispersion is clearly evident. More relevant to the issues discussed here is the observed broadening of the peak as it disperses toward the Fermi level. This was counter to the prevailing notion at the time that the line width was dominated by the photohole lifetime, that is, Im Σ_{e-e}. The experimental angular resolution provides an increasingly important contribution to the observed line width as the band approaches the Fermi level since the Fermi velocity of this state is fairly high (~4 eV/Å^{-1}). However, the apparatus used could control the angular resolution so that its contribution could be extrapolated to zero. There remained a contribution

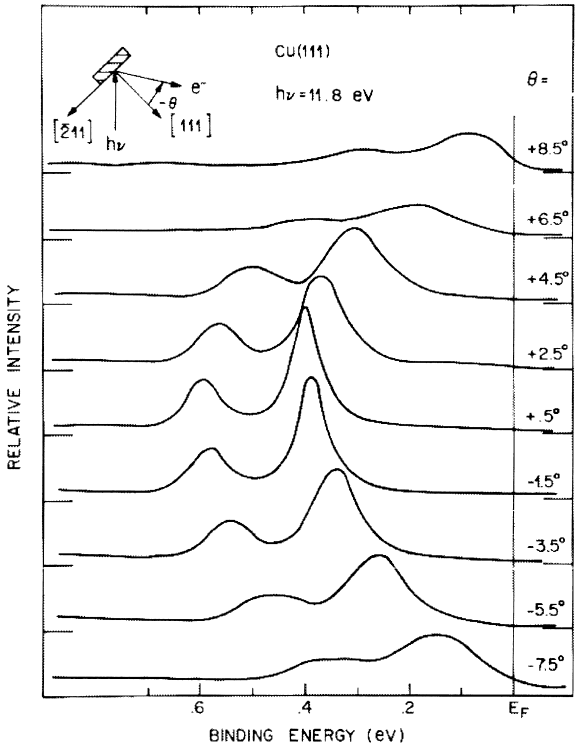

Fig. 3. High resolution photoemission spectra of the Cu(111) surface, seen as doubled due to use of Ar I resonance radiation that consists of two lines. Note the parabolic dispersion about the surface normal which corresponds to the center of the surface Brillouin zone. The peak clearly broadens as it approaches the Fermi level, providing early evidence for the impact of surface impurity and defect scattering (from Ref. [26]).

to the line width that was attributed to impurity scattering — Σ_{imp} in the present context. In actual fact, the broadening was considered to be roughly constant in momentum, not energy, due to a finite mean-free-path due to scattering. Our current understanding would argue otherwise, and it is likely that the early results could be reinterpreted in terms of a constant, pure imaginary Σ_{imp}.

This system was revisited more recently by MacDougall et al. [28] and shortly thereafter by Matzdorf et al. [29], with similar conclusions. They performed experiments with improved energy and momentum resolution and better surfaces. They measured the line width of the surface state at zone center as a function temperature and interpreted their results in terms of (1) a small and constant contribution to the line width from Σ_{imp} and (2) a term due to hole–phonon scattering, Im Σ_{ph}, evaluated within the context of the Eliashberg formalism. Notably absent from their model is any significant contribution to the width from Im $\Sigma_{\mathrm{e-e}}$, which they estimated to be a few meV at the largest hole energy, $\varepsilon_i \sim 400$ meV. This result was at odds with one of the dominant ideas about photoemission line widths at the time. In the Eliashberg or McMillan model, Σ_{ph} is given by [22]

$$\Sigma_{\mathrm{ph}}(\varepsilon) = \int_{-E_{\mathrm{F}}}^{\infty} \mathrm{d}\varepsilon' \int_{0}^{\omega_m} \mathrm{d}\bar{\omega}\alpha^2F(\bar{\omega}) \left\{ \frac{1 - f(\varepsilon',T) + N(\bar{\omega},T)}{\varepsilon - \varepsilon' - \bar{\omega} + i\delta^{\pm}} + \frac{f(\varepsilon',T) + N(\bar{\omega},T)}{\varepsilon - \varepsilon' - \bar{\omega} + i\delta^{\pm}} \right\} \tag{6}$$

where $\alpha^2F(\bar{\omega})$ is the Eliashberg function approximated as a coupling strength multiplied by the phonon density of states, ω_m is the maximum phonon energy ($=\omega_{\mathrm{D}}$ in the Debye model) and sets the energy scale for the interaction, $f(\varepsilon', T)$ is the Fermi–Dirac distribution function, $N(\bar{\omega}, T)$ is the Bose–Einstein distribution function for the phonon gas, and $\delta^{\pm} = \mathrm{sign}(\varepsilon)\delta$ is an infinitesimal. The electron–phonon coupling parameter can be evaluated as

$$\lambda = 2\int_{0}^{\omega_m} \frac{\alpha^2F(\bar{\omega})}{\bar{\omega}}\,\mathrm{d}\bar{\omega} \tag{7}$$

In the Debye model, a straightforward evaluation gives

$$\begin{aligned} \alpha^2F(\omega) &= \lambda\left(\frac{\omega}{\omega_{\mathrm{D}}}\right)^2 \qquad \omega < \omega_{\mathrm{D}} \\ &= 0 \qquad\qquad\quad \text{otherwise} \end{aligned} \tag{8}$$

Eq. (8) can be inserted into Eq. (6) to allow evaluation of $\Sigma_{\mathrm{ph}}(\varepsilon)$ as a function of ε and T in terms of the model parameters λ and ω_{D}. Under many circumstances, Im $\Sigma_{\mathrm{ph}}(\varepsilon, T)$ is nearly independent of energy and linearly dependent on temperature: [28]

$$\mathrm{Im}\,\Sigma_{\mathrm{ph}}(\varepsilon, T) = \pi\lambda k_{\mathrm{B}}T \tag{9}$$

Ignoring the contribution from Im Σ_{e-e}, MacDougall et al. [28], wrote an expression for the photohole quasiparticle line width that included a presumed small constant term from impurity scattering and a term from phonon scattering that depended linearly on temperature. The result of their experiment is shown in Fig. 4, and the fit to the model is clearly quite good. The derived value of λ is 0.14 ± 0.02, a value in reasonable accord with values for bulk copper integrated over the Fermi surface [22]. Note that Im $\Sigma_{ph}(\varepsilon, T)$, in the Debye model and in the limits applied by MacDougall et al. [28], provides no information about the relevant energy scale ω_D, though there is little doubt that, for this system, phonons provide the relevant physics. Also, as noted above, the treatment requires a convolution of effects due to more than one broadening mechanism.

3.3. Electron–phonon coupling and surface superconductivity

The strong coupling theory of superconductivity provides a way to estimate the superconducting transition temperature of a homogeneous system in terms of ω_D, λ, and an effective Coulomb interaction μ^*: [22]

$$k_B T_c = \frac{\hbar\omega_D}{1.45}\exp\left(-\frac{1.04(1+\lambda)}{\lambda-\mu^*(1+0.062\lambda)}\right) \qquad (10)$$

The last of these parameters (μ^*) is difficult to measure, though it does not vary much from ~0.1. Mahan has shown that Eq. (10) is applicable to 2-D systems so long as k_F is not close to a Brillouin zone boundary [30]. The search for high T_c superconductors, prior to the discovery of the cuprates, focused on increasing the characteristic energy scale ω_D and the coupling parameter λ. Unfortunately, these parameters tend to be anticorrelated, with the result that only fairly low T_c was attained through these efforts. Surfaces and interfaces offer a new playground for such efforts that is now augmented by the possibility of measuring these parameters directly using angle-resolved photoemission.

Balasubramanian et al. [31] were the first to make predictions by applying this strong coupling theory to parameters extracted from photoemission measurements. The system they chose was Be(0001). This is a remarkable system in its own right, since the surface is much more metallic than the bulk metal, at least as measured by the density of states at E_F. Using the same techniques described above for Cu(111), they measured λ for a surface band that generates the metallic character, and found it to be several times larger than the bulk value. A simple-minded application of Eq. (10) predicts T_c~70 K, though the authors cautioned that the real T_c would likely be much lower due to the well-known suppression of T_c for a thin superconducting film on a non-superconducting metal substrate [32]. A search for a superconducting gap by Hengsberger et al. [33,34] was unsuccessful, and it currently appears that the surface exhibits normal metallic behavior down to $T=10$ K.

The experiment by Hengsberger et al. [33,34], and a follow-up measurement by LaShell et al. [35], were notable in that they were the first to resolve the impact of Re Σ_{ph} and to use this to measure the interaction energy scale ω_D and the coupling parameter λ. Fig. 5 shows photoemission spectra for the Be(0001) surface state band near the Fermi level, collected with high energy resolution and at low

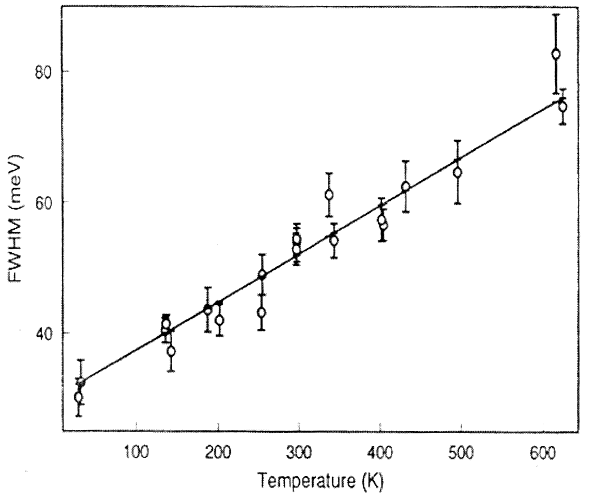

Fig. 4. Observed Lorentzian line width of the Cu(111) zone-center surface states as a function of temperature. The observed linear dependence reflects the phonon contribution to the imaginary part of the hole self-energy. The slope is related to the electron phonon coupling parameter, and was determined to be $\lambda = 0.14\pm0.02$ from these data (from Ref. [31]).

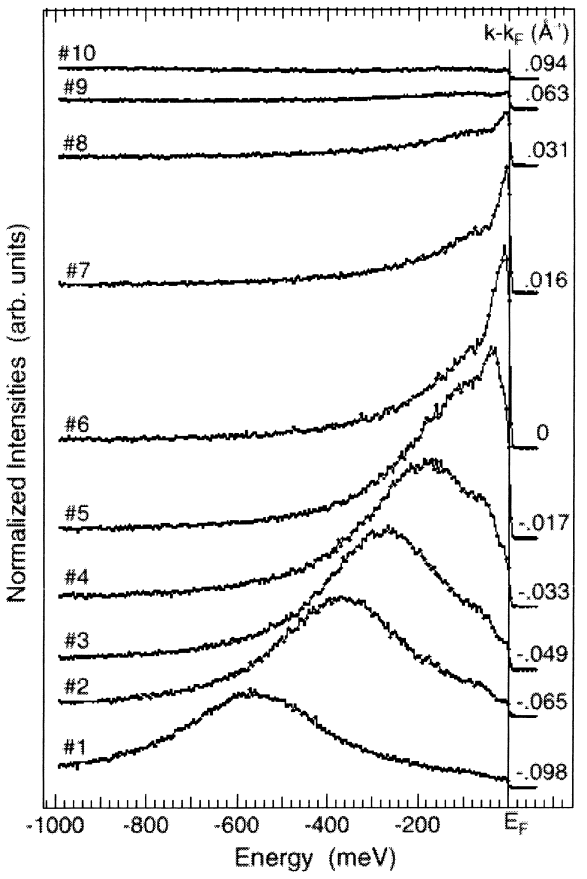

Fig. 5. Photoemission spectra of the Be(0001) surface state at $T=12$ K. The state is relatively broad when at high binding energy, then splits into two peaks near the Fermi level due to mixing between the photohole state and the acoustic phonons. The lower binding energy feature disperses across the Fermi level with notably smaller Fermi velocity due to the phonon enhancement of the band mass. The electron–phonon coupling constant was found to be $\lambda = 1.18 \pm 0.07$ (from Ref. [33]).

temperature [33]. Spectra collected with $k_{\|}$ far from k_F, so that $\varepsilon_i \gg \hbar\omega_D$ (lower spectra), exhibit a single relatively broad feature. As this feature disperses toward $\varepsilon_i \sim \hbar\omega_D \sim 70$ meV, a doubling is clearly visible. A very sharp feature near E_F eventually assumes most of the spectral weight before crossing E_F. Qualitatively, for $\varepsilon_i \gg \hbar\omega_D$, the hole decays efficiently through phonon creation and the quasiparticle is endowed with a shortened lifetime that depends on T. For $\varepsilon_i \ll \hbar\omega_D$, the phase space for inelastic decay is small. Instead, the hole is dressed with a cloud of virtual phonons, and these increase the quasiparticle effective mass. For $\varepsilon_i \sim \hbar\omega_D$ neither situation is valid and the quasiparticle concept actually breaks down — the excitations are of mixed electron–phonon character. A value of λ can be determined by comparing the Fermi velocity to the velocity the band would have in the absence of the electron–phonon interaction, which can be determined by extrapolation of data for $\varepsilon_i \gg \hbar\omega_D$. The ratio of these two is given by $(1+\lambda)$, the well-known electron–phonon mass enhancement [22]. The measured value of λ was in good agreement with the value measured by Balasubramanian et al. [31], using the temperature-dependent line width measurement. Moreover, Hengsberger et al. [33,34], and the later paper by LaShell et al. [35], modeled their spectra directly using Eqs. (2), (3), (6) and (7). A spectral function based on a Debye phonon spectrum provided an excellent representation of their spectra with parameters that provide a reasonable energy scale and a coupling parameter in accord with the previous measurements. A recent experiment by Valla et al. [36], on a surface band on Mo(110) provided similar kinds of observations and conclusions, albeit with less well-defined spectral features due primarily to the reduced Debye temperature for molybdenum as compared to beryllium. In that system, the coupling parameter λ was found to be comparable to the bulk value.

These experiments on Be(0001) and Mo(110) imply that, of all clean metal surfaces, the clearest measurement of both the real and imaginary parts of Σ_{ph} will be observed on the former. The reason for this is that beryllium has the highest Debye temperature of any elemental metal, so the effects are observed at relatively high hole energy scale. However, this is not the whole story since metal surfaces can be modified and engineered, for example, by adsorption of atoms and molecules. These can have higher energy internal and adsorbate-surface vibrations that are known to couple to the electron gas of the substrate. The clearest example of this to date is offered by recent results by Rotenberg et al. [37]. They measured with high resolution the electron–phonon modifications to the surface bands of W(110) with a full monolayer of adsorbed hydrogen. A sampling of their results is presented in Fig. 6. As was seen in Fig. 5 for Be(0001), at relatively high hole energy, a single, relatively broad feature is

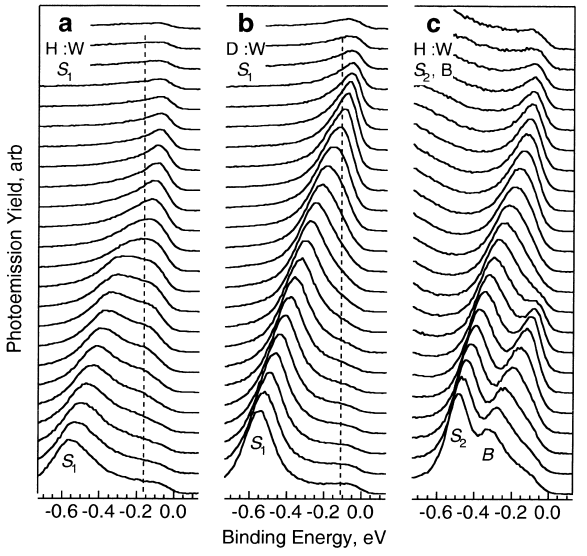

Fig. 6. (a) Detailed spectra for the S_1 surface state for hydrogen on W(110). The splitting of the band near the oscillator energy of the symmetric hydrogen stretching mode (dashed line) is clearly visible. (b) By substituting deuterium for tungsten, the oscillator energy shifts downward due to the H–D isotope effect. The splitting becomes necessarily smaller and shifts upwards towards larger k due to band dispersion, and the spectral features sharpen. (c) By measuring less surface-localized bands having poorer overlap with the adsorbed hydrogen phonon modes, the effects disappear altogether (from Ref. [37]).

observed. As the band approaches E_F, a clear splitting is observed. The characteristic energy can be estimated directly from these spectra, since the action all occurs at hole energy near 150 meV. This is much higher than the bulk tungsten Debye temperature, and corresponds nicely to the energy of the measured symmetric stretching vibration of the hydrogen atoms relative to the surface [38]. This assignment was confirmed with a dramatic deuterium isotope effect, as shown in the middle panel of Fig. 6. Finally, the effect is much reduced for bulk states or less surface-localized surface states (right panel), implying that the perturbing field is indeed localized to the surface. Attempts to fit these spectra to a model spectral function using an Einstein model for the phonon spectrum provided only a qualitative match to the experimental results. The correct way to model these data directly is still being sought. The coupling parameter λ can nonetheless be obtained from the measured Fermi velocity, as was done for Be(0001). A value $\lambda \sim 0.7 \pm 0.3$ was obtained, which is significantly larger than the value for bulk tungsten of 0.2. The surprising aspect of these results is that the system exhibits both a relatively large energy scale, determined by the hydrogen oscillator frequency, and relatively large coupling parameter λ. To date, the system has not been observed to superconduct, though once again a simple-minded application of Eq. (10) would suggest a fairly high T_c.

Compared to conventional superconductivity, where Cooper pairing via electron–phonon coupling has been well understood for decades, the mechanism of pairing in high-T_c superconductors is still hotly debated. A growing body of evidence, however, suggests that the superconducting state is characterized by the coupling between electronic states and their collective spin-excitations. Compared to the metal surfaces discussed above, the superconducting spectral function is complicated by the presence of a Cooper-pair-breaking energy gap. We can get around this problem by considering the Fermi crossing along the direction $k=(0, 0)\rightarrow(\pi, \pi)$ in the surface Brillouin zone, because, owing to the d-wave nature of the pairing, there is no gap along this nodal direction. Hence an ordinary Fermi crossing can be observed both in normal and superconducting states in this direction.

For this crossing, it has been recently observed in BSCCO compounds [6,39] that for $T < T_c$ a 'kink' develops in the dispersion curve, in a manner qualitatively similar to that for the metal surface states discussed above. A weak 'peak-dip-hump' lineshape near E_F in the nodal direction continuously strengthens as one moves from the nodal direction towards $(0, \pi)$. Such spectra look strikingly similar to the data near E_F for the Be surface state illustrated in Fig. 5 (albeit with the additional presence of the superconducting gap at E_F). In the context we have been discussing, it is therefore natural to consider these results to be a consequence of the coupling between electronic states and an excitation which appears only for $T < T_c$. Indeed such a mode with an appropriate energy scale and momentum dependence has been observed in BSCCO by neutron scattering [40]. A complete accounting of the ARPES spectral function throughout the entire Brillouin zone is likely to be a constraint on any theory of the fundamental

excitations in the system, which are intimately related to the mechanism of high-T_c superconductivity.

3.4. Surface screening phenomena at $q = 2k_F$

The results from the previous sections pertain largely to electron–phonon coupling at $q = 0$. That is, in Fig. 1, dominant degeneracy and strongest couplings occur near $q = 0$ and $\omega = 0$. The modified electron self-energy leads to a reduced Fermi velocity, a precursor to gap formation. This has led naturally to the notion that we might be able to form Cooper pairs and a superconducting ground state using a traditional coupling mechanism in distinctly non-traditional media. As mentioned in the introduction, however, there is an entirely different set of coupling phenomena at low energy associated with $q = 2k_F$. These can lead to screening singularities and anomalies in the dispersion relations of low energy excitations and to charge- or spin-density wave distorted ground states. In the context of surface physics, such screening phenomena have been proposed to cause surface reconstruction [41] and to mediate the lateral interaction between adsorbed particles [42,43] and between surface steps [44], through mechanisms closely related to the RKKY interaction in bulk media.

Charge-density wave phenomena have been proposed to explain observations in a few different surface adsorption systems [45,46], and recently evidence for an antiferromagnetic spin-density wave ground state for one monolayer of Mn adsorbed on W(110) has been presented [47]. Also, for the first time the bulk spin-density-wave band gap in chromium has been measured with angle-resolved photoemission [48]. From the context of the present review, however, these systems are not yet as precisely understood as, for example, electron–phonon coupling on the Be(0001) where a direct measure of the coupling strength has been achieved by careful analysis of the photoemission spectra. The underlying changes in electronic structure are relatively small, and excepting the experiment on bulk chromium a detailed measure of the evolution of the charge-density-wave or spin-density-wave band gap as a function of wave vector and temperature has not yet been achieved. Indeed, the interpretation of Carpinelli et al. [45], of an observed reconstruction on Sn/Ge(111) in terms of a charge-density-wave has been called into question since the measured Fermi contours apparently do not support the observed periodicity [49,50]. The (4×1)In–Si(111) system exhibits pronounced one-dimensionality and thus should be more prone to electronic instabilities. The measured Fermi surface matches the observed periodicity doubling, though the underlying band gap has not yet been studied in detail [46]. At present the understanding of the underlying 'many body effects' at these surfaces is less complete than for the systems discussed above.

A system where '$2k_F$ physics' seems to play a key role is W(110)+H. Early measurements of the Fermi contours for this system [51] motivated detailed phonon measurements that detected a pronounced anomaly in the Rayleigh mode along the $\bar{\Sigma}$ azimuthal direction at a wave vector $q = 0.93$ Å^{-1}. The relevant phonon dispersion relations are shown in the left panel of Fig. 7 [52,53]. The source of an anomaly this well localized in *k*-space is almost certainly 'nesting' between different portions of the surface Fermi contours. The term nesting refers to the condition when separate segments of the Fermi contours have similar curvature and parallel tangents. In this case the phase space for electron–hole pair creation at the vector that connects the two segments is large and the generalized susceptibility can be large. Elementary excitations in the system at the nesting wave vector and at low energy will be strongly screened by (i.e., strongly coupled to) the electron–hole pair continuum. In slightly different language, this is a generalization of the physics leading to the cusp near $q = 2k_F$ in Fig. 1b. If the screening is strong enough, the coupled mode can become soft and the system reconstructs through a charge- or spin-density-wave mechanism. Apparently the screening in W(110)+H is not strong enough to cause a reconstruction, but a pronounced anomaly is observed nonetheless.

Unfortunately, the early Fermi contour measurements for the hydrogen-covered surface had a systematic error and it did not at first appear that appropriately nested segments existed on the surface. Subsequent calculations of the Fermi contours showed segments that were appropriately nested [54–57], calling the early experimental results into

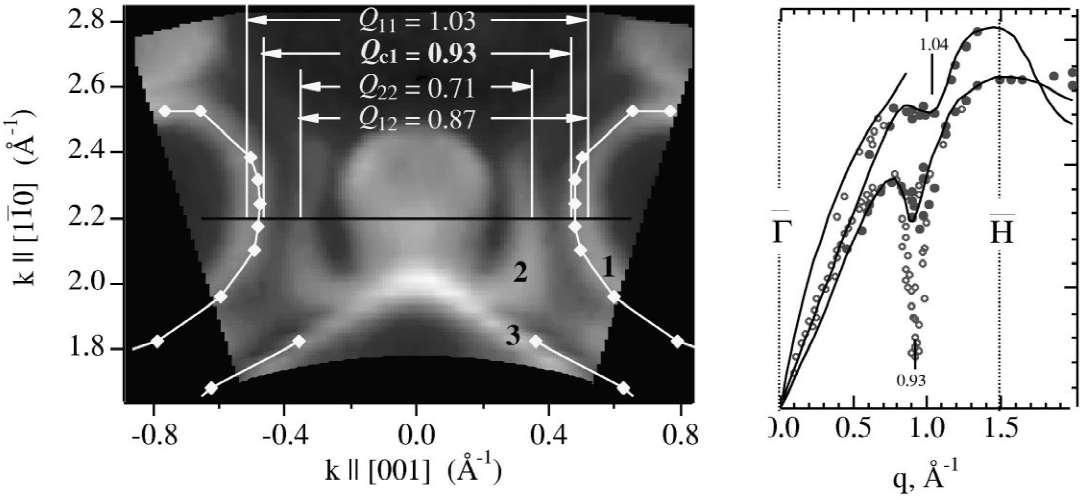

Fig. 7. Right panel: Surface phonon dispersion relations for W(110) with a monolayer of adsorbed hydrogen along the Σ azimuthal direction (experimental data from Ref. [53]; solid lines are from the calculation in Ref. [56]). Note the distinct softening of the Rayleigh mode at $q = 0.93\text{Å}^{-1}$ in addition to a weaker anomaly observed in a higher energy branch. Left panel: The relevant portion of the experimental surface Fermi contours for the same surface, indicating possible nesting vectors that might be responsible for the observed anomaly (experimental data from Ref. [58]; lines and symbols are from the calculation in Ref. [54]). Based on the location of the observed anomaly alone (Q_{c1}), the most likely vector couples segments 1 and 2, Q_{12}. The segments are derived from the same band that is split by the spin–orbit interaction.

question. The photoemission experiments were done again with higher sensitivity and resolution and with more systematic technique [58]. The newer results showed good nesting at the appropriate wave vector, but with an interesting twist. As indicated in the left panel of Fig. 7, the contour implicated in the calculations as being responsible for the anomaly was found to be significantly split into two bands labelled S_1 and S_2. The splitting was attributed to the impact of the spin–orbit interaction in the presence of the surface, which breaks inversion symmetry. Indeed, an unusual spin structure was predicted to exist on this surface in which the orientation of the spin evolves smoothly so as always to be orthogonal to the surface normal and the Fermi contour [59]. This spin structure helps to determine the position of the phonon anomaly, since the electron–phonon interaction is spin-independent and thus cannot couple states of opposite spin. In the future, it will be useful and interesting to measure the quasiparticle dispersion relations for states that are strongly nested with high resolution and at low temperature, where the interaction between lattice modes, spin, and electron states dominates.

4. Observations and conclusions

The various articles in this special issue collectively document the rebirth being experienced by angle-resolved photoemission. This rebirth is probably not measured in terms of the number of practitioners, which seems in any case to be a monotonically increasing function of time. Rather it has been spawned by the development of high resolution spectrometers and associated instruments that allow investigations of quasiparticle dispersion relations at a scientifically important level of detail. This is perhaps most clearly true, for example, in oxide materials that are often referred to as ‘complex’, where photoemission is playing a key role in elucidating the mechanism of high temperature superconductivity and colossal magnetoresistance. One of our goals in writing this paper, however, is to indicate that complex and interesting phenomena occur in ‘simple’ systems. Consider the W(110) surface, for example. By any measure, this is an extremely well-studied surface. Surface science essentially started many decades ago on W(110). Nonetheless, in the past several years, it has become

apparent that (1) a surface band is split by the spin–orbit interaction to produce a strange magnetic structure that is ordered in *k*-space, (2) the Fermi contour produced by this spin-split band is well-nested and thereby causes a deep anomaly in surface phonon dispersion relations, and (3) the coupling of the very same band to hydrogen adsorbate vibrations is anomalous as measured by the combined strength of the interaction and the magnitude of the energy scale. Much of this new phenomenology was motivated and measured by high resolution angle resolved photoemission.

It is unlikely that progress in developing this new phenomenology will end with W(110) and related surfaces. It is probable that surfaces that exhibit phenomena distinctly different from the bulk will be those with large projected gaps at the Fermi level. In this case, there will tend to be a sizable surface-localized density of states, a prime criterion for supporting exotic phenomena. Among elemental metals, the group IIA and the group VIB metals are prototypical in this regard. It is, therefore, no surprise that much of the initial developments discussed in this paper were done on beryllium and tungsten.

Acknowledgements

This work was supported by the US DOE under grant DE-FG06-86ER45275.

References

[1] G. Grüner, Density Waves in Solids, Addison-Wesley, Reading, MA, 1994.
[2] J. Solyom, Adv. Phys. 28 (1979) 201.
[3] Z.X. Shen, J.R. Schrieffer, Phys. Rev. Lett. 78 (1997) 1771.
[4] M.R. Norman, H. Ding, J.C. Campuzano et al., Phys. Rev. Lett. 79 (1997) 3506.
[5] A. Abanov, A.V. Chubakov, Phys. Rev. Lett. 83 (1999) 1652.
[6] A. Kaminski, J. Mesot, H. Fretwell et al., Phys. Rev. Lett. 84 (2000) 1788.
[7] C.-O. Almbladh, L. Hedin, Theory of photoemission, in: E.E. Koch (Ed.), Handbook of Synchrotron Radiation, North-Holland, Amsterdam, 1983, p. Vol. 16.
[8] W. Bardyszewski, L. Hedin, Phys. Script. 32 (1985) 439–450.
[9] L. Hedin, J. Phys: Condensed Matter 11 (1999) R489–R528.
[10] J.E. Inglesfield, Phys. Script. 117 (1987) 89–92.
[11] J.E. Inglesfield, J. Phys. C: Solid State Phys. 16 (1983) 403.
[12] J.E. Inglesfield, E.W. Plummer, Physics of photoemission, in: S.D. Kevan (Ed.), Angle-Resolved Photoemission, Elsevier, Amsterdam, 1992, p. 15.
[13] M.S. Hybertsen, S.G. Louie, Comments Condens. Matter Phys. 13 (1987) 223.
[14] M.S. Hybertsen, S.G. Louie, Phys. Rev. Lett. 55 (1985) 1418.
[15] M.S. Hybertsen, S.G. Louie, Phys. Rev. B 34 (1986) 5390.
[16] S. Hüfner, Photoelectron Spectroscopy, Springer, Berlin, 1995.
[17] R. Claessen, R.O. Anderson, J.W. Allen et al., Phys. Rev. Lett. 69 (1992) 808.
[18] S. Hüfner, R. Claessen, F. Reinert et al., J. Elect. Spectroscopy 100 (1999) 191–213.
[19] L. Hedin, S. Lundqvist, Jellium theory, in: F. Seitz, D. Turnbull, H. Ehrenreich (Eds.), Solid State Physics, Vol. 23, Holt, Reinhardt, and Winston, New York, 1969, p. 1.
[20] D. Pines, P. Nozières, The Theory of Quantum Liquids, Benjamin, New York, 1969.
[21] A. Beckmann, K. Meinel, M. Heiler et al., Phys. Status Solidi B 198 (1996) 665.
[22] G. Grimvall, The Electron–Phonon Interaction in Metals, North-Holland, New York, 1981.
[23] E. Jensen, E.W. Plummer, Phys. Rev. Lett. 55 (1985) 1912–1915.
[24] I.-W. Lyo, E.W. Plummer, Phys. Rev. Lett. 60 (1988) 1558.
[25] L. Hedin, Phys. Rev. 139 (1965) 796.
[26] P. Thiry, D. Chandesris, J. Lecante, et al., Phys. Rev. Lett. 82 (1979).
[27] S.D. Kevan, Phys. Rev. Lett. 50 (1983) 526.
[28] B.A. McDougall, T. Balasubramanian, E. Jenses, Phys. Rev. B 51 (1995) 13891.
[29] R. Matzdorf, G. Meister, A. Goldmann, Phys. Rev. B 54 (1996) 14807.
[30] G.D. Mahan, Phys. Rev. B 48 (1996) 16557.
[31] T. Balasubramanian, E. Jensen, X.L. Wu et al., Phys. Rev. B 57 (1998) R6866.
[32] P.G. de Gennes, Rev. Mod. Phys. 36 (1964) 225.
[33] M. Hengsberger, D. Purdie, P. Segovia et al., Phys. Rev. Lett. 83 (1999) 592–595.
[34] M. Hengsberger, R. Fresard, D. Purdie et al., Phys. Rev. B 60 (1999) 10796–10802.
[35] S. LaShell, E. Jensen, T. Balasubramanian, Phys. Rev. B 61 (2000) 2371–2374.
[36] T. Valla, A.V. Fedorov, P.D. Johnson et al., Phys. Rev. Lett. 83 (1999) 2085–2088.
[37] E. Rotenberg, J. Schaefer, S.D. Kevan, Phys. Rev. Lett. 84 (2000) 2925.
[38] M. Balden, S. Lehwald, H. Ibach, Phys. Rev. B 53 (1996) 7479.
[39] T. Valla, A.V. Fedorov, P.D. Johnson et al., Science 285 (1999) 2110.
[40] H.F. Fong, P. Bourges, Y. Sidis et al., Nature 398 (1999) 588.
[41] E. Tosatti, Solid State Commun. 25 (1978) 637–640.
[42] K.H. Lau, W. Kohn, Surface Sci. 75 (1978) 69–85.
[43] N.H. March, Prog. Surface Sci. 25 (1987) 229–251.

[44] W. Xu, J.B. Adams, T.L. Einstein, Phys. Rev. B 54 (1996) 2910–2916.
[45] J.M. Carpinelli, H.H. Weitering, E.W. Plummer et al., Nature 381 (1996) 398–400.
[46] H.W. Yeom, S. Takeda, E. Rotenberg et al., Phys. Rev. Lett. 82 (1999) 4898.
[47] S. Heinze, M. Bode, A. Kubetza et al., Science 288 (2000) 1805–1808.
[48] J. Schäfer, E. Rotenberg, S.D. Kevan et al., Phys. Rev. Lett. 83 (1999) 2069.
[49] J. Avila, Y. Huttel, A. Mascaraque et al., Surface Sci. 435 (1999) 327–331.
[50] J. Avila, A. Mascaraque, E.G. Michel et al., J. Elect. Spect. 103 (1999) 361–365.
[51] R.H. Gaylord, K. Jeong, S.D. Kevan, Phys. Rev. Lett. 62 (1989) 203.
[52] E. Hulpke, J. Lüdecke, Surface Sci. 287/288 (1993) 837–841.
[53] E. Hulpke, J. Lüdecke, Phys. Rev. Lett. 68 (1992) 2846–2849.
[54] B. Kohler, P. Ruggerone, S. Wilke et al., Phys. Rev. Lett. 74 (1995) 1387.
[55] B. Kohler, P. Ruggerone, S. Wilke et al., Zeitschrift f. Physikalische Chemie 197 (1996) 193.
[56] C. Bungaro, S.D. Gironcoli, S. Baroni, Phys. Rev. Lett. 77 (1996) 2491.
[57] K.W. Kwak, M.Y. Chou, N. Troullier, Phys. Rev. B 53 (1996) 13734–13739.
[58] E. Rotenberg, S.D. Kevan, Phys. Rev. Lett. 80 (1998) 2905.
[59] E. Rotenberg, S.D. Kevan, submitted to Phys. Rev. Lett. (1998).